Available online at www.sciencedirect.com
ScienceDirect
Catalysis Today 130 (2008) 272–282
CATALYSIS TODAY
www.elsevier.com/locate/cattod

Genesis of new HDS catalysts through a careful control of the sulfidation of both Co and Mo atoms: Study of their activation under gas phase

Naïma Frizi [a], Pascal Blanchard [a], Edmond Payen [a,*], Pascale Baranek [a], Michael Rebeilleau [b], Carole Dupuy [b], Jean Pierre Dath [b]

[a] *Unité de Catalyse et de Chimie du Solide, UMR CNRS 8181, Université des Sciences et Technologies, 59655 Villeneuve d'Ascq, France*
[b] *Total Petrochemicals Research, Zone industrielle CB-7181, Feluy, Belgium*

Abstract

Impregnation of oxidic precursor with thioglycolic acid aqueous solution was successfully used to improve the performances of thiophene hydrodesulfurization catalysts. Raman, EXAFS and XPS studies indicate that addition of this chelating agent affects the sulfidation of the supported metals. The higher catalytic performances were attributed to an optimization of the nature and morphology of the active phase obtained by the use of this chelating agent which permits a simultaneous sulfidation of both Co and Mo atoms.

Keywords: Hydrotreatment; MoS_2; Thiophene; Sulfidation; CoMo; Catalysts; HDS; Complexing agent; Morphology

1. Introduction

The new severe environmental regulations concerning the reduction of sulfur content in diesel oil impose a drastic improvement of the hydrodesulfurization (HDS) of petroleum feedstocks which is a catalytic process most generally performed on $CoMo/Al_2O_3$ catalysts. These active catalysts are obtained by sulfiding an oxidic precursor that is generally prepared by incipient wetness impregnation of an alumina support with an aqueous solution containing Co and Mo salts followed by a drying and a calcination step. It is now well recognized that the active phase is the CoMoS one which consists of well dispersed MoS_2 nanocrystallites decorated with the Co promotor atoms which are located at their edges and corners [1]. The catalyst preparation is therefore a key step for achieving high activities, particularly to avoid any loss of cobalt atom in the alumina support thus forming $CoAl_2O_4$-type species which are hardly sulfidable [2]. These Co atoms are no use to promote the molybdenum disulfide slabs. Moreover, during the sulfidation inactive bulk Co_9S_8 entities may also be formed which is also detrimental to the activity. During these last years new methods of preparation of the oxidic precursors have been developed with the goal to improve the catalytic performances of these solids. The addition of organic chelating agents in the impregnating solutions used for the preparation of these alumina supported (Ni)CoMo-based oxidic precursors underwent a rapid development. Whatever the nature of the chelating agent and the thermal treatment, several hypotheses have been proposed to explain their exact role. But in all cases it was stated that they contribute to optimize the formation of the CoMoS phase through

(i) an improvement of the Mo and/or Co dispersion [2–9] and a decrease of the Co fraction in the cobalt aluminate phase [2],
(ii) the modification of the relative rates of sulfidation of Co and Mo atoms [10–18],
(iii) a diminution of the interaction between the metals and the support [19–24].

A new approach for improving the performances of hydrotreating catalysts with the use of various organic agents has been developed in our laboratory [25]. It consists of impregnating a conventional $CoMo(P)/Al_2O_3$ oxidic precursor which has yet been calcined with a solution containing the organic agent. In the present study we first propose to use

* Corresponding author.
E-mail address: edmond.payen@univ-lille1.fr (E. Payen).

0920-5861/$ – see front matter
doi:10.1016/j.cattod.2007.10.109

thioglycolic acid (TGA) aqueous solution, a chelating agent which can also be used as a sulfiding compound such as patented by the Sumitomo Mining Company [26]. After the preparation of the so-modified oxidic precursors, a detailed characterization of the genesis of the active phase is presented. Then the improvement of the catalytic performances in HDS of thiophene of the modified catalyst is correlated to the nature and the morphology of the active phase as deduced from the aforementioned study of the sulfidation, which allows us to understand the exact role of this chelating agent.

2. Experimental

2.1. Preparation of the oxidic precursors

The $CoMo/Al_2O_3$ catalyst used in this work is a calcined commercial one with 18 wt% as MoO_3 and 3.5 wt% as CoO. This oxidic precursor will be denoted herafter as CoMoRef.

For comparison purposes a Mo/Al_2O_3 oxidic precursor was prepared by incipient wetness impregnation of a commercial γ-Al_2O_3 (water pore volume: 1 $cm^3\ g^{-1}$; specific surface area: 350 $m^2\ g^{-1}$) with an ammonium heptamolybdate (AHM) aqueous solution, the AHM concentration being chosen to prepare a 20 MoO_3 wt% solid, a value which corresponds to the same Mo surface density as the $CoMo/Al_2O_3$ catalyst. Similarly a Co/Al_2O_3 oxidic precursor was prepared by impregnation of the γ-Al_2O_3 with an aqueous solution containing cobalt nitrate and ethylenediamine according to the method described by Blanchard et al. [2–4]. This method allowed us to prepare a solid with a Co loading of 4 wt% as CoO without formation of any bulk Co_3O_4. The impregnated extrudates were then dried at 100 °C overnight and calcined in air at 500 °C for 4 h. The Mo/Al_2O_3 and the Co/Al_2O_3 oxidic precursors are respectively denoted as MoRef and CoRef.

2.2. Preparation of the modified oxidic precursors

The modified oxidic precursors were prepared by incipient wetness impregnation of the CoMoRef, CoRef and MoRef with an aqueous solution containing the desired amount of thioglycolic acid. After 2 h of maturation the so obtained modified solids were dried at 80 °C under N_2 during 15 h but were not calcined. Several TGA/Mo molar ratios were studied and these modified catalysts are denoted Mo*X*TGA, and CoMo*X*TGA where *X* is the TGA/Mo molar ratio. In the case of the Co/Al_2O_3-based solid, the modified solids are denoted Co*X*TGA but for comparison purposes the amounts of TGA impregnated correspond to those added for CoMo*X*TGA.

2.3. Sulfided catalysts

For characterizations, the oxidic precursors were sulfided at temperatures ranging between 50 and 350 °C. The sulfidation was performed at atmospheric pressure with a flow (100 mL/min) of H_2/H_2S (90/10) mixture in glass reactors equipped with a cell which permits the Raman spectroscopic analysis without any transfer of the sample. The sulfidation temperature rate was 6 °C min^{-1} up to the desired temperature and the sample were eventually further maintained at this temperature as stated. After sulfidation the reactors were closed and immediately cooled down. They were then placed in a glove box under argon in order to avoid any reoxidation of the solids during the sampling of the XPS and EXAFS analysis.

2.4. Catalytic activities

Catalytic activities in thiophene HDS were measured at atmospheric pressure in a flow-bed reactor packed with 200 mg of catalyst. The reactor is designed to work under differential conditions. The catalysts were first sulfided at 350 °C for 3 h under a flow (100 mL min^{-1}) of a H_2S/H_2 (10/90) mixture in the catalytic reactor. Then the temperature was cooled down to 270 °C for the evaluation of thiophene HDS conversion. After purification by vacuum distillation, thiophene was introduced in the reactor at constant pressure (50 Torr) in a flow of purified hydrogen (10 mL min^{-1}). The reaction products (butane and butenes) were analysed by gas chromatography. At the conversions studied in this work the HDS rate can be calculated by $r = \alpha\, D_{thio}/m$ where D_{thio} is the flow of thiophene, m the mass of the catalyst and α is the thiophene conversion [27]. As the density of the different catalysts is not constant due to the addition of TGA, the reaction rate is expressed per gram of catalyst corrected by the loss of ignition.

2.5. Characterizations

2.5.1. X-ray photoelectron spectroscopy (XPS)

XPS sampling was performed under argon atmosphere in a glove box. The powdered samples were pressed into an indium foil attached to the sample holder which was introduced directly in the XPS spectrometer thanks to the connection of the glove box to the XPS transfer chamber of the spectrometer. XPS spectra were recorded with the VG ESCALAB 220 XL spectrometer equipped with a monochromatic Al Kα (E = 1486.6 eV) X-ray source. The spectra were collected with a pass energy of 30 eV using the electromagnetic lens mode low-energy electron flood gun for charge compensation effect. The binding energies (BE) of Mo 3d, Co 2p, C 1s and S 2p were determined by computer fitting of the measured spectra and referred to the Al 2p photopic of the support at 74.6 eV. The binding energies were estimated to be within ±0.2 eV. The surface atomic ratios $I_{Mo\ 3d}/I_{Al\ 2p}$ and $I_{Co\ 2p}/I_{Al\ 2p}$ were calculated using the VG Eclipse software after subtracting the non-linear Shirley background and the contribution of the S 2s signal to the Mo 3d signals. The Mo 3d and Co 2p spectra were decomposed using an interactive least-squares program and the fitting peaks of the experimental curves were defined thanks to a combination of Gaussian (70%) and Lorentzian (30%) distributions. These decompositions were performed to quantify the fraction of Mo and Co which was chelated by TGA after modification of the oxidic precursor and to estimate after sulfidation the percentages of Mo atoms which form the MoS_2 slabs and of Co atoms implied in the sulfide phase (i.e. CoMoS + Co_9S_8). These percentages will be hereafter noted

''Mo sulfidation degree'' and ''Co sulfidation degree''. The surface quantification is based on the surface peaks area relative to each chemical species present on the surface of the solid.

The decompositions of the Mo 3d spectra have been performed simulating each contribution with two peaks corresponding to the Mo $3d_{5/2}$ and Mo $3d_{3/2}$ core levels and taking into account that the binding energy difference BE(Mo $3d_{5/2}$) − BE(Mo $3d_{3/2}$) is equal to 3.15 eV, the Mo $3d_{5/2}$/Mo $3d_{3/2}$ peak area ratio is equal to 1.5 and the full width at half maximum (FWHM) of the Mo $3d_{5/2}$ and Mo $3d_{3/2}$ peaks are almost the same [28–31]. The S 2s peak which contributes to the total envelope of the spectra of Mo 3d was simulated with only one peak by taking as reference the S 2p peak with respect to the following criteria: BE(S 2s) − BE(S 2p) = 64 eV. For the modified oxidic precursors, the methodology implemented for the decompositions is as follows. The contribution of the oxide state has been determined from the analysis of the reference oxidic precursor. This contribution has been introduced in the spectra of the modified solids. Other contributions were then introduced, their number depending on the shape of the spectra to be decomposed. Fig. 1A shows an example of such decomposition that will be commented hereafter. For the sulfided catalysts, the Mo 3d spectrum have been decomposed into the three well known contributions respectively attributed to Mo^{VI} oxide (BE = 233.0 eV), Mo^{V} oxysulfide (BE = 230.5 eV) and Mo^{IV} (MoS_2) (BE = 228.8 eV) [28] (Fig. 1B).

Due to the complexity of the Co 2p spectrum (multiplet effect, satellites structures) [29], the methodology implemented has consisted of isolating successively the contributions of each Co-based chemicals species. Each contribution has been simulated with four peaks corresponding to the Co $2p_{3/2}$ (main peak + satellite structure) and Co $2p_{1/2}$ (main peak + satellite structure) core levels. For each contribution, the spectral parameters (BE differences, intensity ratios and FWHM ratios) of these four peaks are interdependent for all the decompositions. This enables to decompose the spectra by varying only the global intensity of each contribution to obtain the relative amount of each species. Fig. 2 shows examples of decomposition of the Co 2p spectra after modification of the oxidic precursor and after sulfidation of the catalyst. For each spectrum, two contributions were used considering only the presence of two states for Co atoms, i.e. Co^{2+} in oxide state and Co^{2+} chelated by TGA or Co^{2+} in sulfur environment as will be discussed hereafter.

The absence of any signal at 169.0 eV (characteristic of sulfates) indicates that no re-oxidation of the sulfided catalysts

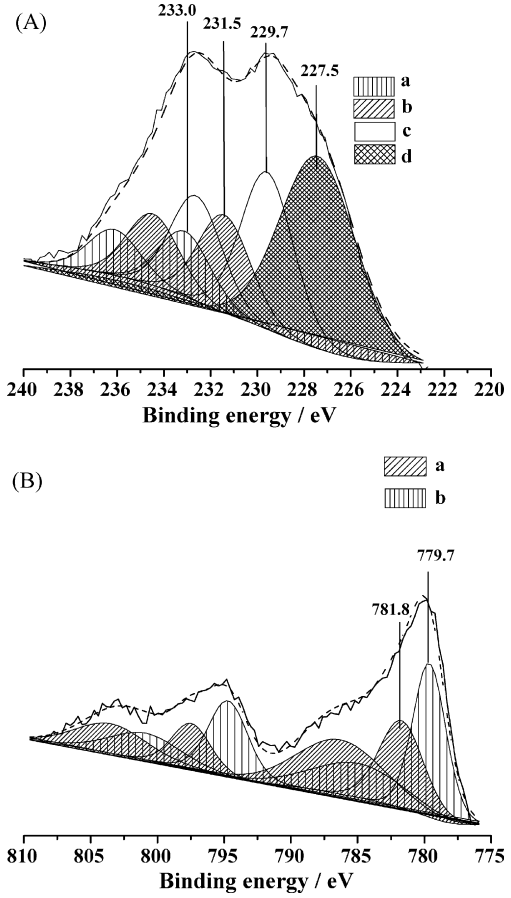

Fig. 1. Decomposition of the Mo 3d and Co 2p XPS spectra of CoMo4TGA. (A) Mo 3d XPS spectrum: (a) contribution of the Mo^{VI} oxidic phase; (b) and (c) contributions of the Mo^{V}–TGA entities; (d) contribution of S 2s. (B) Co 2p XPS spectrum: (a) contribution of the Co^{II} oxidic phase; (b) contribution of the Co–TGA entity.

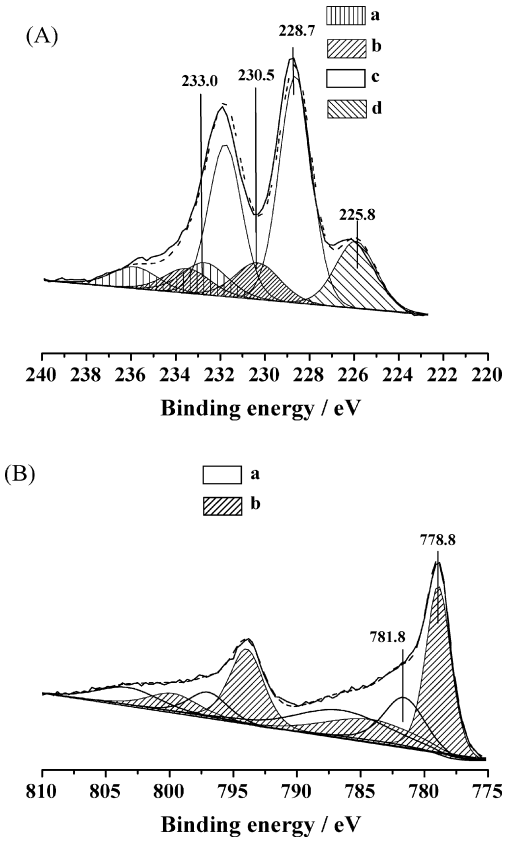

Fig. 2. Decomposition of the Mo 3d and Co 2p XPS spectra of CoMo4TGA after sulfidation (H_2/H_2S, 90/10) at 350 °C for 3 h. (A) Mo 3d XPS spectrum: (a) contribution of the Mo^{VI} oxidic phase; (b) contribution of the Mo^{V} oxysulfide phase; (c) contribution of the $Mo^{IV}S_2$ phase; (d) contribution of the S 2s. (B) Co 2p XPS spectrum: (a) contribution of the Co^{II} oxidic phase; (b) contribution of the Co atoms in sulfidic phases.

occurred during the transfer of the solid from the sulfiding reactor to the XPS machine.

2.5.2. X-ray absorption spectroscopy

Mo and Co K-edge extended X-ray absorption fine structure (EXAFS) measurements of the oxidic precursors were carried out at the BM30B (FAME) beam line at the European Synchrotron Radiation Facility (ESRF, Grenoble, France). The energy of the beam line is 6 GeV with an average current of 200 mA. The EXAFS data were taken in the transmission mode through a double crystal monochromator Si (1 1 1) using two ion chambers as detectors. The samples were analysed by transmission mode. For each sample, the accumulation time was about 30 min at the Mo K-edge with three recorded spectra and about 40 min at the Co K-edge with five recorded spectra. EXAFS oscillations $\chi(k)$ were extracted from the raw data using the Athena program [32]. The Fourier transform (FT) of the $k^3\chi(k)$ signal was performed over the 2.825–13 Å^{-1} and 3–9.581 Å^{-1} K-ranges respectively for the Mo K-edge and the Co K-edge to obtain the so-called radial distribution pseudo-function. The sampling pellets were prepared in a glove box by mixing the catalyst with cellulose, the amount of catalyst being calculated to obtain an absorption jump equal to 1 and a total absorption inferior to 3.

2.5.3. Raman spectroscopy

The Raman spectra of the samples, maintained at room temperature, were recorded using a Raman microprobe (Infinity from Jobin-Yvon) equipped with a photodiode array detector. The exciting laser source was the 532 nm line of a Nd-YAG laser with a power of the beam of 0.23 mW at the focal point. The wavenumber accuracy was 2 cm^{-1}.

2.5.4. High-resolution electron microscopy (HREM)

High-resolution electron microscopy was performed on a TECNAI TEM (200 kV) equipped with a LaB_6 filament. Freshly sulfided samples were ground under an inert atmosphere and were dispersed in heptane. The suspension was collected on a microscope grid covered with a thin carbon holed film. For statistical analysis more than 20 photographs were taken, which enabled us to measure about 2000 slabs for each sample. Statistical analysis of each photograph was done by measuring the length (L) and stacking (N) of the MoS_2 slabs.

3. Results

3.1. Reactivity

Thiophene HDS rates obtained for the CoMoRef and CoMo4TGA catalysts are reported in Table 1. It shows that the modification of the conventional oxidic precursor by TGA induces an increase of the catalytic performances in HDS of thiophene. Moreover, the improvement depends on the amount of chelating agent added, the best improvement being obtained with a TGA/Mo ratio of 4. Physico-chemical characterizations of this modified oxidic precursor have been performed at each step of the genesis of the active catalyst with the goal to understand the exact role of this agent.

Table 1
Catalytic performances in HDS of thiophene for the studied solids

Catalysts	Thiophene HDS rate (mol s^{-1} g^{-1})
CoMoRef	2.44×10^{-8}
CoMo2TGA	4.88×10^{-8}
CoMo4TGA	6.00×10^{-8}

3.2. Characterization of modified oxidic precursors

3.2.1. Raman spectroscopy

It is well admitted that thioglycolic acid forms complexes with molybdenum by chelating the metal via the SH and COOH groups [33–35] but very few studies have been published on the complexation of Co atoms with thiols [36,37]. To evidence the formation of Mo–TGA and/or Co–TGA complexes upon modification, Raman characterizations have been performed. Fig. 3 shows the Raman spectra of the reference and of the modified catalyst in the 200–1600 cm^{-1} range. For comparison the spectrum of an aqueous TGA solution is also presented. The spectra of CoMoRef and MoRef catalysts do not exhibit the features of bulk oxides such as MoO_3 or $CoMoO_4$ while they exhibit a main line at 950 cm^{-1} which is characteristic of the presence of well dispersed polymolybdate species [38]. Diffuse reflectance UV–vis spectroscopy also shows the absence of bulk Co_3O_4. Indeed the UV–vis spectrum of CoMoRef (not reported here) does not present the characteristic bands of this entity [3]. The spectra of the modified solids are very different from those of the oxidic precursors. The spectrum of CoMo4TGA exhibits Raman lines at 260, 377 cm^{-1} and two lines at 950 and 962 cm^{-1}. The intense lines at 260 and 377 cm^{-1} are also observed in the spectrum of Co4TGA. These lines are respectively assigned to Co–S and Co–O stretching modes in Co–TGA complexes by reference to the literature data [25,39]. The spectrum of Mo4TGA presents two main lines at

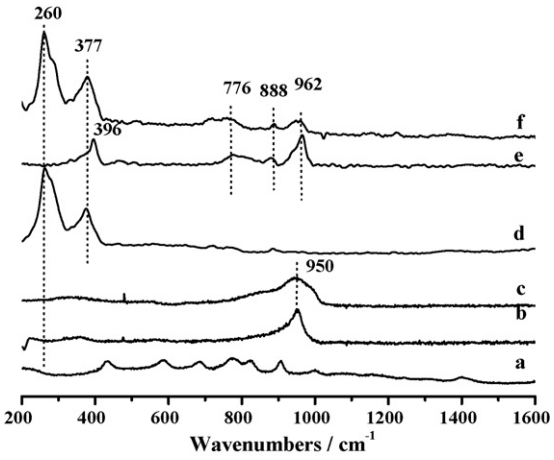

Fig. 3. Raman spectra in the 200–1600 cm^{-1} spectral range of (a) TGA aqueous solution; (b) MoRef; (c) CoMoRef; (d) Co4TGA; (e) Mo4TGA; (f) CoMo4TGA.

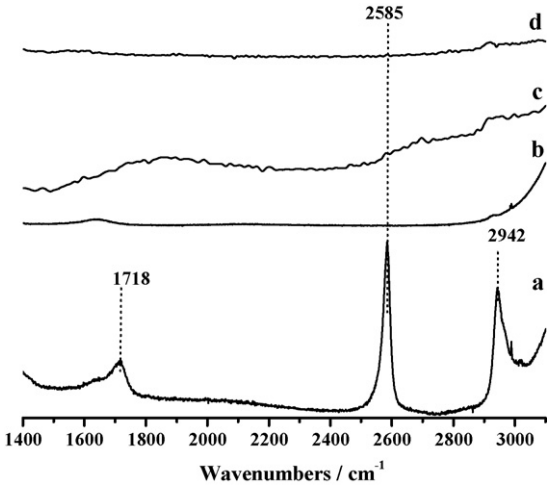

Fig. 4. Raman spectra in the 1400–3100 cm^{-1} spectral range of (a) TGA aqueous solution; (b) Mo4TGA; (c) Co4TGA; (d) CoMo4TGA.

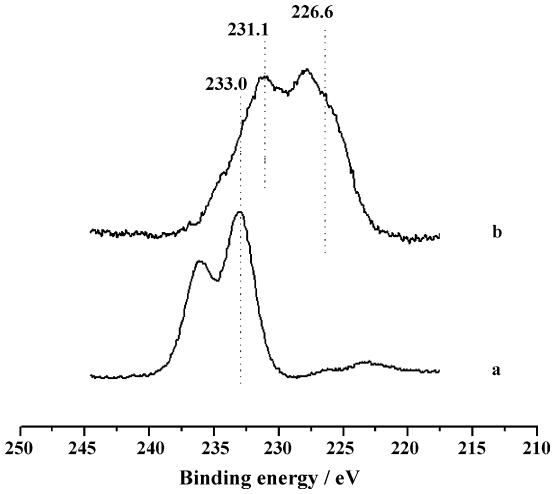

Fig. 5. Mo 3d XPS spectra of (a) CoMoRef; (b) CoMo4TGA.

396 and 962 cm^{-1} (with a remaining one at 950 cm^{-1}) which are respectively assigned to Mo–S and Mo–O vibrations in Mo–TGA complexes [25,40–43]. Considering the relative intensities of the lines at 260, 377, 396 and 960 cm^{-1}, the lines at 396 cm^{-1} is probably masked by the more intense lines at 377 cm^{-1} in the spectrum of CoMo4TGA. Even if the observation of the Raman lines at 950 cm^{-1} indicates that some polymolybdates species remained intact, these spectra show that new Mo- and Co-based species are formed upon modification with TGA. Moreover, the lines characteristic of the TGA solution are not observed in the spectra of Mo4TGA, Co4TGA and CoMo4TGA which is confirmed in the high wavenumbers range. Indeed, Fig. 4 shows the Raman spectra of these samples in the 1400–3100 cm^{-1}. The Raman spectrum of the TGA aqueous solution exhibits lines at 2585 (very strong), 1718 and 2942 cm^{-1} which are respectively assigned to the S–H stretching mode, the carbonyl stretching mode of the carboxylic group and the CH_2 groups [44]. In the Mo4TGA, Co4TGA and CoMo4TGA spectra, these Raman lines are no longer observed. This change indicates that all the TGA molecules are coordinated to the catalysts, the excess of TGA being evacuated during the drying at 80 °C under nitrogen as suggested by thermogravimetric analysis [45].

To conclude, the Raman characterizations indicate that new Mo–TGA and Co–TGA complexes are formed upon impregnation of the oxidic precursors with thioglycolic acid.

3.2.2. XPS

Figs. 5 and 6 show respectively the Mo 3d and Co 2p spectra of the CoMoRef and CoMo4TGA samples. The Mo 3d spectrum of the reference oxidic precursor exhibits a Mo $3d_{5/2}$ photopic with an apparent binding energy (BE) equal to 233.0 eV, which is characteristic of Mo^{VI} in oxide environment. The introduction of TGA induces a strong change of the Mo 3d spectrum shape. This results in a shift in the apparent BE and a drastic broadening of the XPS photopeaks. This suggests the presence of Mo^{V} species in which the metal is bonded to oxygen and sulfur. Indeed in most of the Mo–TGA-based complexes described in the literature data the Mo atoms are in this oxidation state [34]. The decomposition of the Mo 3d spectrum of the modified solid has been performed to quantify the proportion of Mo–TGA species. As shown in Fig. 1A, three contributions are necessary to obtain the best simulation of the experimental spectrum. The first introduced one corresponds to the starting Mo^{VI} species of the oxidic precursor (BE = 233 eV). The two others, the Mo $3d_{5/2}$ BE of which are respectively 231.5 and 229.7 eV, are attributed to Mo^{V} atoms chelated by TGA [25], the peak at BE = 227.5 eV being due to the S 2s contribution. This allows us to estimate that 75% of the Mo atoms are chelated by TGA. This is in agreement with the Raman data which show that some polymolybdates species are still present after modification of the oxidic precursor.

The Co 2p spectrum of the non-modified catalyst exhibits the features of cobalt in oxide environment with the Co $2p_{3/2}$ peak at 781.8 eV and a shake up satellite at higher binding energies. The introduction of TGA induces a decrease of the BE

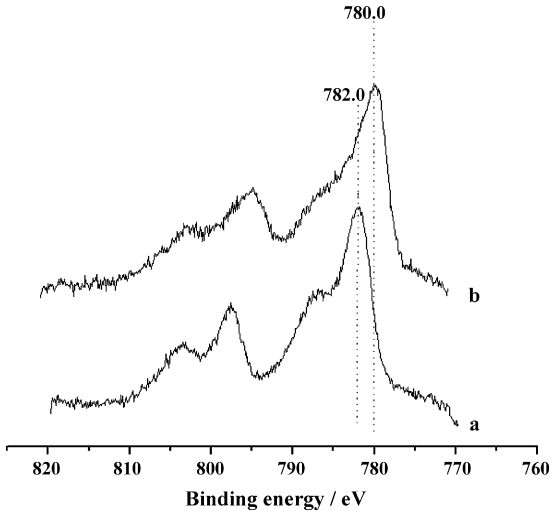

Fig. 6. Co 2p XPS spectra of (a) CoMoRef; (b) CoMo4TGA.

Table 2
Dispersion of Mo and Co for the CoMoRef and CoMo4TGA solids before and after sulfidation at 350 °C under H_2/H_2S as determined by XPS

Samples	$I_{Mo\ 3d}/I_{Al\ 2p}$	$I_{Co\ 2p}/I_{Al\ 2p}$
CoMoRef	1.50	0.89
CoMo4TGA	1.37	1.02
Sulfided CoMoRef	1.70	1.16
Sulfided CoMo4TGA	1.61	1.13

of the Co $2p_{3/2}$ peak, which is assigned to the formation of Co–TGA complexes. For the decomposition of the Co 2p spectrum of the CoMo4TGA solid, two contributions are identified. They respectively correspond to Co atoms in oxidic state (Co $2p_{3/2}$ BE = 781.8 eV) and Co atoms chelated by TGA (Co $2p_{3/2}$, BE = 779.7 eV) [25]. It also appears that 50% of the Co atoms are chelated by TGA.

The dispersion of the metals, represented by the intensity ratios $I_{Mo\ 3d}/I_{Al\ 2p}$ and $I_{Co\ 2p}/I_{Al\ 2p}$, has been calculated for each solid. These ratios are reported in Table 2. No significant variations are induced by the modification indicating that the dispersion of the Mo and Co is not affected by the addition of TGA on the oxidic precursor.

3.3. Characterization of the catalysts during the sulfidation

3.3.1. Raman spectroscopy

Fig. 7 shows the Raman spectra of the CoMo4TGA after sulfidation at different temperatures. No modification is observed after activation at 110 °C during 3 h, the Raman spectrum being quite similar to the spectrum of the starting modified oxidic precursor. The main lines (at 260 and 960 cm^{-1}) characteristic of the presence of Mo–TGA and Co–TGA entities are still observed, which suggests that these entities are preserved after this treatment. Very weak lines are also observed in the 400–550 cm^{-1} region, which characterises the presence of a small amount of oxysulfide entities [46]. After sulfidation at 220 °C for 3 h the relative intensities of the lines characteristic of the Mo–TGA and Co–TGA species drastically decrease. Moreover, the spectrum exhibits additional lines at 380, 330, 431 and 537 cm^{-1} which can be assigned to the aforementioned Mo oxysulfide species similar to those observed during the sulfidation of a conventional CoMo catalyst [46]. This indicates that the Mo–TGA and Co–TGA species are partially sulfided after the treatment at 220 °C for 3 h.

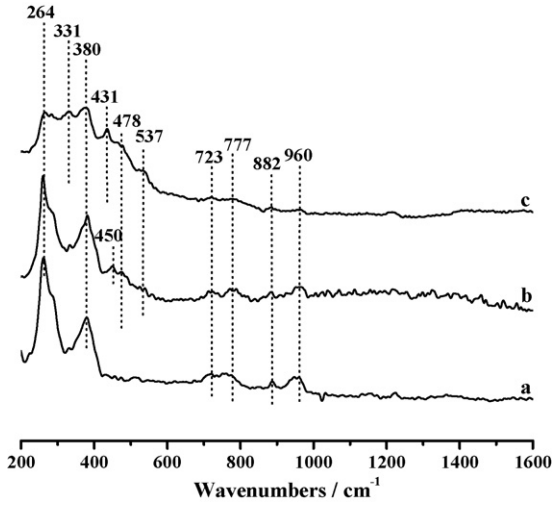

Fig. 7. Raman spectra of CoMo4TGA in the 200–1600 cm^{-1} spectral range after sulfidation (H_2/H_2S, 90/10) at various temperatures: (a) unsulfided; (b) 110 °C, 3 h; (c) 220 °C, 3 h.

3.3.2. EXAFS

The local structures of Mo and Co atoms have been studied by EXAFS at the same steps of the sulfidation. The k^1-weighted EXAFS signal and the k^3-weighted Fourier transform modulus (FT) which were derived from the Mo K-edge and the Co K-edge EXAFS spectra of the CoMoRef and CoMo4TGA catalyst before and after sulfidation at 110 and 220 °C for 3 h are respectively presented in Figs. 8–11.

For the reference solid, the FT modulus at the Mo K threshold (Fig. 8) consists of three peaks at 1.15, 1.80 and 2.75 Å (without phase correction) which mainly characterise Mo–O and Mo–Mo contributions in this type of solid [47–49]. Upon increasing the temperature, molybdenum is sulfided as shown by the strong reduction of the amplitude of the Mo–O contribution. On the other hand, the amplitude of a peak at 1.85 Å corresponding to a Mo–S contribution increases. These results are in agreement with the works of Leliveld et al. as well as Parham et al. which evidence a progressive sulfidation of the Mo starting in

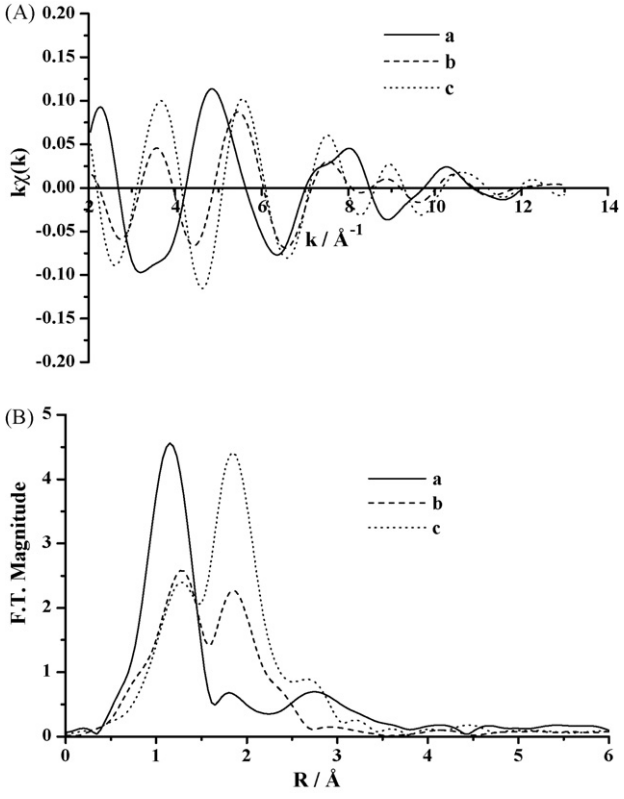

Fig. 8. (A) k^1-weighted EXAFS signals; (B) k^3-weighted Fourier transform modulus (2 825–13 $Å^{-1}$) for Mo K-edge of CoMoRef after sulfidation (H_2/H_2S, 90/10) at various temperatures—(a) unsulfided; (b) 110 °C, 3 h; (c) 220 °C, 3 h.

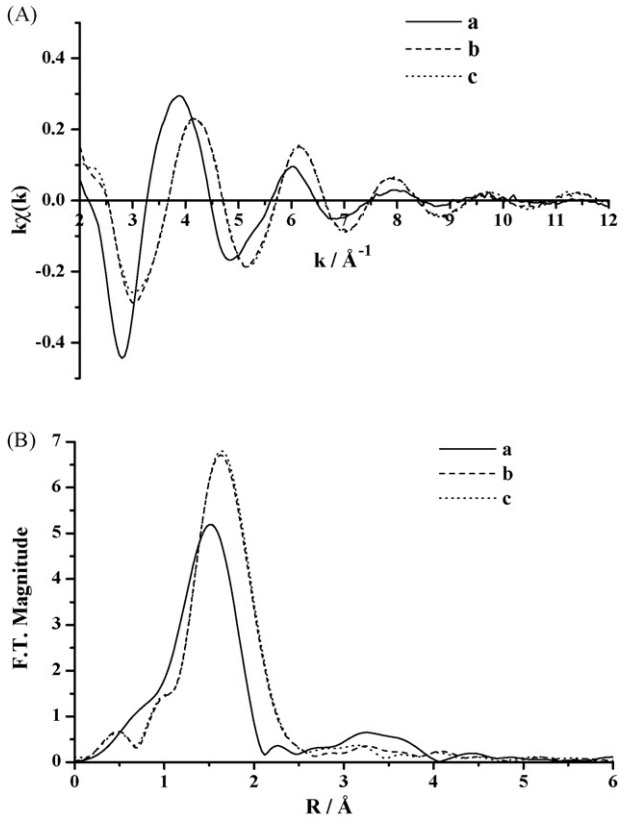

Fig. 9. (A) k^1-weighted EXAFS signals; (B) k^3-weighted Fourier transform modulus (2–8.581 Å^{-1}) for Co K-edge of CoMoRef after sulfidation (H_2/H_2S, 90/10) at various temperatures—(a) unsulfided; (b) 110 °C, 3 h; (c) 220 °C, 3 h.

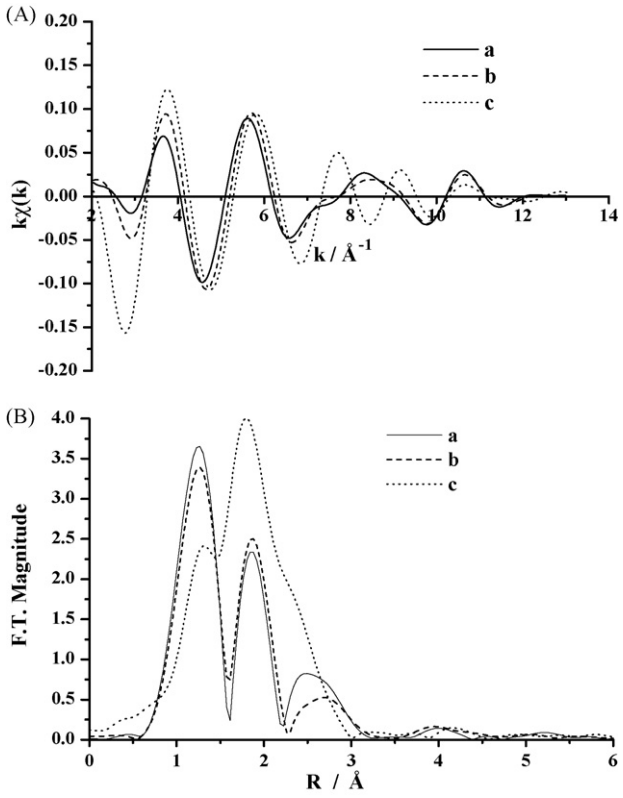

Fig. 10. (A) k^1-weighted EXAFS signals; (B) k^3-weighted Fourier transform modulus (2.825–13 Å^{-1}) for Mo K-edge of CoMo4TGA after sulfidation (H_2/H_2S, 90/10) at various temperatures—(a) unsulfided; (b) 110 °C, 3 h; (c) 220 °C, 3 h.

temperatures ranging between 75 and 100 °C. The FT modulus of the fresh sample at the Co K threshold presents one peak at 1.51 Å which characterises the Co–O contribution (Fig. 9). Evolution of the FT modulus during the various treatments points out a sulfidation of the Co atoms. Indeed, at 110 °C an increase of the amplitude of the peak at 1.64 Å corresponding to a Co–S contribution [50] is observed. Thus it appears that the FT modulus at the Mo K threshold evolves after each treatment while it does not change between 110 and 220 °C at the Co K threshold.

The signals and FT modulus obtained at the Mo K threshold of the CoMo4TGA are very different from those obtained for CoMoRef. The FT modulus of the modified oxidic precursor (Fig. 10) exhibits three peaks at 1.5, 1.8 and 2.3 Å (without phase correction) which originate from the several Mo-based species present at the surface of the alumina. The sulfidation of Mo in this solid is also different. Indeed, in agreement with the aforementioned Raman results, the signals of the modified oxidic precursor before and after sulfidation at 110 °C are nearly similar confirming that only a small amount of Mo atoms are sulfided at low temperature. On the other hand, after the treatment at 220 °C the amplitude of the second peak of the Mo K FT modulus increases whereas the amplitude of the first one decreases. Accordingly this should correspond to the sulfidation of the Mo–TGA species. Very similar results are obtained with the Co–TGA species. Indeed, the signals and the FT modulus obtained at the Co K threshold of the fresh catalyst and sulfided at 110 °C are similar (Fig. 11). They present one shell at 1.7 Å which results from the Co-based species present after addition of TGA. At 220 °C the decrease of the peak amplitude implies, in accordance with the evolution of the Raman spectrum, the decomposition of the Co–TGA species upon sulfidation.

3.3.3. XPS

All the aforementioned results suggest that the TGA chelated species are stable under the activation conditions at low temperature. Thus it is very interesting to know how the sulfidation of both molybdenum and cobalt is affected. Figs. 12 and 13 present the evolution of the Co 2p XPS spectra of the CoMoRef and CoMo4TGA catalysts at different steps of the activation. After sulfidation at 350 °C, all the spectra exhibit a main peak at about 778.7 eV characteristic of Co in sulfur environment [51]. During the activation of CoMoRef, the Co 2p spectrum evolves continuously from low temperatures to 220 °C. Indeed, the intensity of the oxidic state Co contribution (BE = 781.8 eV) decreases while the sulfidic state Co one increases. So the cobalt sulfidation starts at ambient temperature and seems complete after 3 h at 220 °C. Moreover, the evolution of the XPS spectra shows that the Co is already almost completely sulfided at 110 °C in agreement with the EXAFS results.

For CoMo4TGA the evolution is very different. Indeed, the spectrum of the Co 2p is similar to the modified starting oxidic

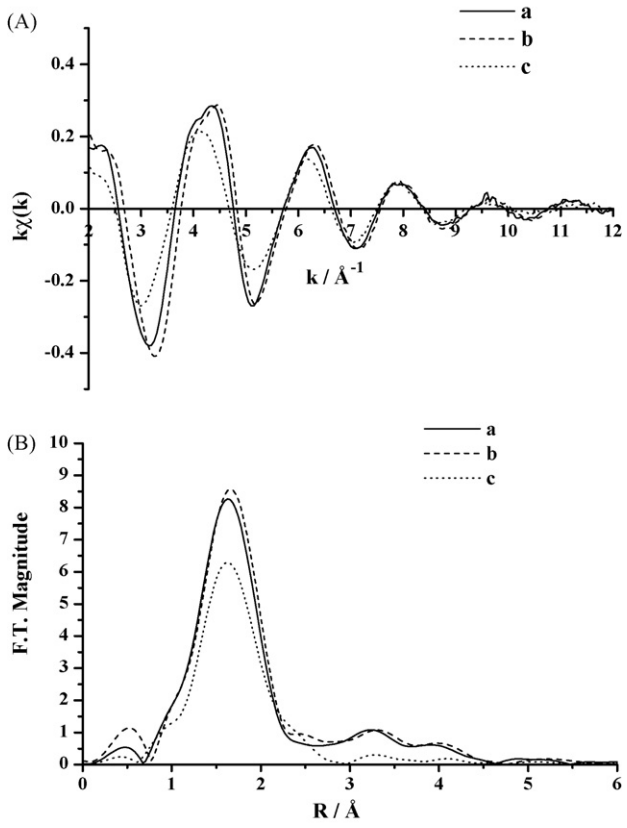

Fig. 11. (A) k^1-weighted EXAFS signals; (B) k^3-weighted Fourier transform modulus (2–8.581 Å^{-1}) for Co K-edge of CoMo4TGA after sulfidation (H_2/H_2S, 90/10) at various temperatures—(a) unsulfided; (b) 110 °C, 3 h; (c) 220 °C, 3 h.

precursor up to 220 °C. Therefore, the Co–TGA species stability permits to avoid any cobalt sulfidation before 220 °C, this sulfidation starting during the stage at 220 °C as shown by the shift of the Co $2p_{3/2}$ BE. However, the sulfidation appears complete after treatment at 350 °C. Indeed, the BE of this main peak shifts continuously from 780.0 to 778.6 eV between 220 and 350 °C in agreement with a decrease of its full width at half maximum.

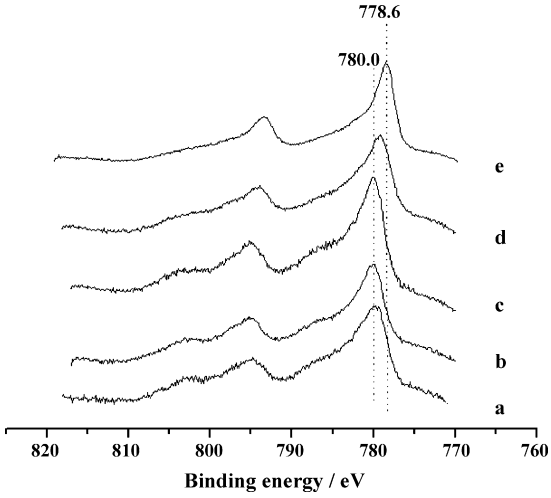

Fig. 13. Co 2p XPS spectra of CoMo4TGA after sulfidation (H_2/H_2S, 90/10) at various temperatures: (a) unsulfided; (b) 110 °C, 3 h; (c) 220 °C, without stage; (d) 220 °C, 3 h; (e) 350 °C, 3 h.

Figs. 14 and 15 show the evolution of the Mo 3d XPS spectra of the CoMoRef and CoMo4TGA catalysts at the same steps of sulfidation. Whatever the solid after sulfidation at 350 °C, the spectra of Mo 3d core level are similar and exhibit respectively a Mo $3d_{5/2}$ photopic at 228.7 and 228.5 eV characteristic of MoS_2, the shoulder at BE = 225.8 eV being due to the S 2s photopeak. Concerning CoMoRef, the Mo XPS features of the oxide components (peaks at 233 and 236.1 eV) gradually disappear while those of the sulfide ones appear (peaks at 228.5 and 231.6 eV) upon increasing the sulfidation temperature from room temperature up to 350 °C. Thus, molybdenum sulfidation starts at room temperature and finishes at 350 °C. For CoMo4TGA, only a small change of the Mo 3d spectrum is observed before 220 °C in accordance with the aforementioned Raman and EXAFS results. This can be explained by taking into

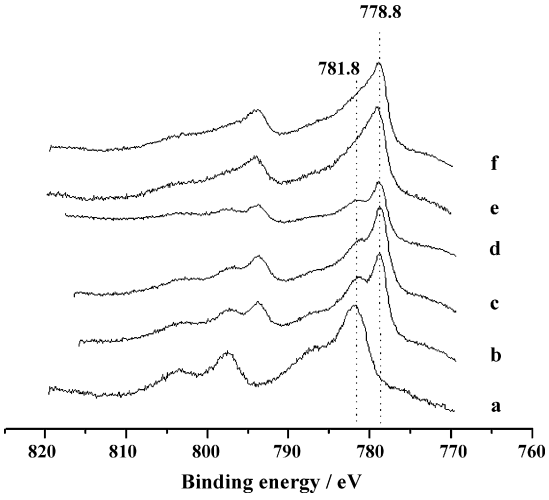

Fig. 12. Co 2p XPS spectra of CoMoRef after sulfidation (H_2/H_2S, 90/10) at various temperatures: (a) unsulfided; (b) 50 °C, 1 h; (c) 110 °C, 3 h; (d) 220 °C, without stage; (e) 220 °C, 3 h; (f) 350 °C, 3 h.

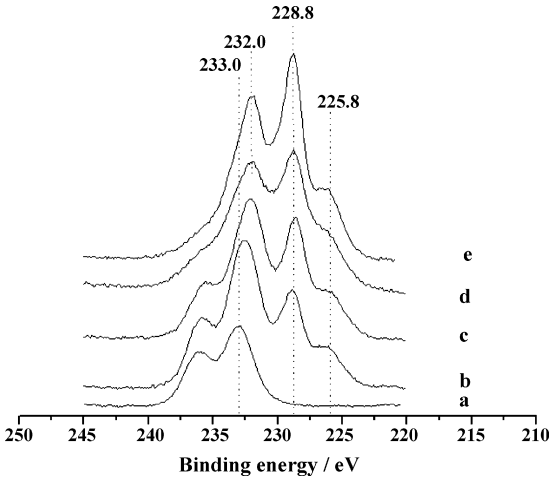

Fig. 14. Mo 3d XPS spectra of CoMoRef after sulfidation (H_2/H_2S, 90/10) at various temperatures: (a) unsulfided; (b) 50 °C, 1 h; (c) 110 °C, 3 h; (d) 220 °C, 3 h; (e) 350 °C, 3 h.

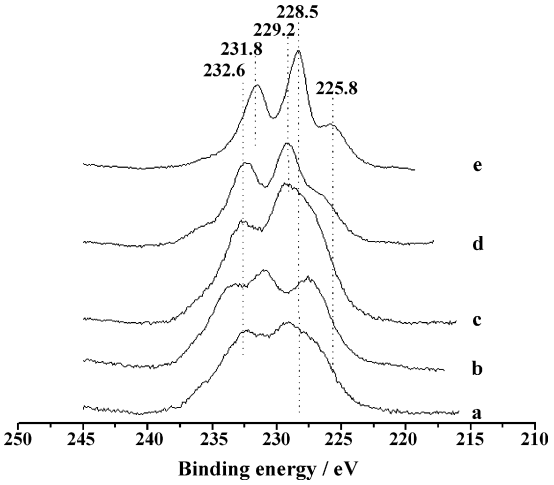

Fig. 15. Mo 3d XPS spectra of CoMo4TGA after sulfidation (H_2/H_2S, 90/10) at various temperatures: (a) unsulfided; (b) 110 °C, 1 h; (c) 220 °C, without stage; (d) 220 °C, 3 h; (e) 350 °C, 3 h.

account the evolution during the sulfidation of the C 1s core level XPS peak at 289 eV which characterises the TGA carboxyl group (not shown here). Its intensity remains constant up to 220 °C and starts to decrease during the stage at 220 °C. This confirms that the TGA-based entities are preserved up to 220 °C, their decomposition starting during the stage at this temperature. Consequently, in agreement with the Raman and EXAFS results, only a small amount of non-chelated molybdenum atoms are sulfided at temperatures lower than 220 °C. Then the Mo 3d spectrum evolves and evidences the sulfidation of the molybdenum atoms upon increasing the temperature up to 350 °C. Thus this study shows that the sulfidation of Co is achieved before that of Mo in the CoMoRef as already observed by several authors [10–12,17,18] while the sulfidation of both Mo–TGA and Co–TGA species occurs simultaneously in the same range of temperatures, i.e. from 220 to 350 °C.

The nature and dispersion of the active phase of solids sulfided at 350 °C have also been examined. The binding energy differences BE(Co $2p_{3/2}$) − BE(S 2p) and BE(Co $2p_{3/2}$) − BE(Mo $3d_{5/2}$) presented in Table 3 characterise whatever the catalyst cobalt atoms mainly in decoration position of the MoS_2 phase according to Topsøe et al. [51]. Moreover, Table 2 shows that the dispersion of the active metals after sulfidation is not affected by the chelating agent as indicated by the constant values of the $I_{Co\ 2p}/I_{Al\ 2p}$ and $I_{Mo\ 3d}/I_{Al\ 2p}$ ratios. Nevertheless, the shape of the XPS spectra of Co 2p and Mo 3d core level after sulfidation at 350 °C of CoMo4TGA indicates that TGA induces a better sulfidation of molybdenum and cobalt atoms. Accordingly, a decomposition of the XPS Mo 3d and Co 2p peaks (Fig. 2A and B) has been performed for both catalysts with the aim to evaluate the Mo and Co sulfidation degrees which are reported in Table 3. For the decomposition of the Co 2p spectra of the sulfided solids two contributions, the Co $2p_{3/2}$ BE of which being 781.8 and 778.7 eV, were used. They respectively correspond to Co atoms in oxide state and Co atoms in sulfide state. This decomposition shows that the modification with TGA induces an increase of both Co and Mo sulfidation degrees.

Table 3
XPS data of the CoMoRef and CoMo4TGA catalysts sulfided at 350 °C and morphology of the MoS_2 slabs

Catalysts	CoMoRef	CoMo4TGA
BE(Co $2p_{3/2}$) − BE(Mo $3d_{5/2}$) (eV)	550	550.1
BE(Co $2p_{3/2}$) − BE(S 2p) (eV)	617	616.8
Co sulfidation percentage (%)	45	60
Mo sulfidation percentage (%)	60	67
Average stacking of the MoS_2 slabs	1.7	1.5
Average length of the MoS_2 slabs (Å)	33	27

3.3.4. Electron microscopy

Fig. 16 presents one of the HREM photographs obtained for the sulfided catalysts. The statistical analysis of these photographs is summed up in Table 3. This table shows that the modification of the reference by TGA induces a different morphology of the active phase. Indeed while the stacking of the MoS_2 slabs of the CoMoRef and the CoMo4TGA are similar, the modification by TGA induces a decrease of the length of these slabs.

4. Discussion

It has thus been shown that the impregnation of a classical CoMo-based oxidic precursor with TGA aqueous solution induces a large improvement of the thiophene HDS conversion. The active phase remaining the CoMoS one, the improvement of the catalytic performances should be explained by the modification of the CoMoS phase induced by the use of TGA.

Firstly, XPS results show that no increase of the dispersion of the ''oxidic phase'' is provided by the modification with TGA. Indeed the $I_{Mo\ 3d}/I_{Al\ 2p}$ and $I_{Co\ 2p}/I_{Al\ 2p}$ ratios remain constant upon TGA impregnation. This implies that the dispersion of the metals is not affected by the formation of the TGA complexes. However, the dispersion was already optimized on the oxidic precursor as no bulk oxide (MoO_3, $CoMoO_4$, Co_3O_4) was identified by Raman and UV spectroscopy before the addition of the TGA-modifying agent. Thus, contrarily to previous studies where the objective was to improve the dispersion by the introduction of chelating agents in the impregnating solution [2–9], here the objective is to change the nature of the supported species that will be activated by sulfidation. Indeed, whatever the complexing agent used in these studies, a calcination step was performed before the sulfidation. Consequently this was always the same type of oxomolybdate species which were sulfided, the calcination being a levelling step for these modifications [2].

Secondly, the modification of CoMoRef by TGA provokes an enhancement of the molybdenum sulfidation degree. It means that a larger amount of Mo atoms are implied in the formation of MoS_2 slabs. This induces that a higher number of MoS_2 slabs and therefore a higher number of active sites are generated on the modified catalysts since the TEM study has shown that the length of the crystallites decreases upon addition of TGA. The complexation with TGA is at the origin of this

higher sulfidation degree thanks to the decrease of the Mo–alumina interaction or to the modification of the nature of the supported species that will be activated by sulfidation. The same effect is observed for the cobalt atoms. Indeed, the TGA induces a higher cobalt sulfidation degree which should also be considered to explain the improvement of the performances. This increase of the cobalt sulfidation degree implies that more Co atoms would be available for the decoration of the MoS_2 edges. It can be suggested that some Co^{2+} atoms of the aforementioned $CoAl_2O_4$ surface species, which are supposed to be hardly sulfidable, are used for the promotion thanks to the chelating agent.

Moreover, after the sulfidation cobalt atoms can be present in the CoMoS active phase [52] or as Co_9S_8 microcrystallites, the formation of these latter being detrimental to the promoting effect. We showed in this work that the sulfidation of both Mo and Co is nearly simultaneous thanks to the similar stability of Mo–TGA and Co–TGA species versus the sulfidation. This permits to retard the sulfidation of cobalt and thus to inhibit the formation of Co_9S_8 allowing to have more Co atoms in the decoration position. Indeed, several authors proposed that the improvement of the HDS performances obtained through the use of complexing agents (En, EDTA, CyDTA or NTA, etc.) [10–18] for the preparation of oxidic precursors could be assigned to the modification of the genesis of the active (Ni)CoMoS phase if the catalysts were not calcined before the sulfidation. Indeed, if the sulfidation of Co(Ni) proceeds after the formation of the MoS_2 slabs, the Co ions are able to disperse themselves over the edges of the MoS_2 crystallites. On the opposite, without any complexing agent the sulfidation of Co would be complete before the formation of MoS_2 slabs, yielding bulk Co_9S_8 which is not able to promote the MoS_2 slabs at higher temperatures.

But the simultaneity of the sulfidation of both Co and Mo atoms can also be related to the decrease of the MoS_2 slabs size which is evidenced for the CoMo4TGA. Indeed, the simultaneity of the migration of the Co atoms on the MoS_2 edges during the formation of the disulfide slabs and their growth should decrease their size. This is in agreement with DFT calculations showing that sulfur atoms have a lower affinity to cobalt than to molybdenum [53]. So the presence of cobalt atoms in decoration position over MoS_2 crystallite edges would prevent the growth of the slabs. On the contrary, if the cobalt atoms are blocked against sulfidation by a chelating agent whereas molybdenum sulfidation takes place, the MoS_2 slabs will consequently be longer than without chelating agent. This is in agreement with the results recently obtained by Gonzalez-Cortés et al. which show that an increase of the MoS_2 size is observed upon sulfidation of a $CoMo/Al_2O_3$ oxidic precursor prepared with EDTA in such amount that only the Co atoms are chelated [54].

5. Conclusion

This work confirms that the sulfidation of a conventional HDS CoMo catalyst is not optimized. Indeed, the sulfidation of Co is finished whereas all the Mo atoms are not yet transformed into MoS_2. We clearly show in this study that the catalytic performances of such a conventional oxidic precursor can be improved through its modification by impregnation of a chelating agent such as thioglycolic acid. The genesis of the active phase upon sulfidation has been studied with the aim to understand the exact role of this complexing agent. It has been shown that addition of TGA on a commercial CoMo oxidic precursor where the dispersion of metals was already optimized has no effect on the dispersion of the metals. The improvement of the performances is assigned to the complexation of the Mo and Co atoms with TGA which induces

- the increase of the sulfidation degree of the active metals,
- the simultaneous sulfidation of the Mo and Co atoms which leads to a decrease of the MoS_2 slabs length as well as an increase of the number of Co atoms in decoration position.

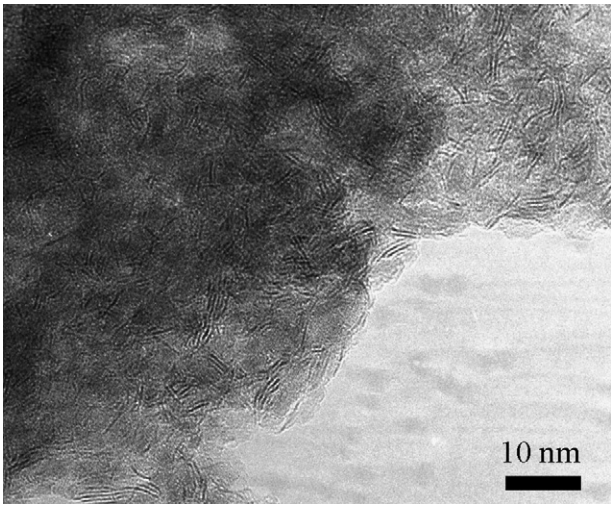

Fig. 16. Typical HREM micrograph of sulfided CoMo4TGA.

References

[1] H. Topsøe, B.S. Clausen, F.E. Massoth, Hydrotreating Catalysis, Springer, Berlin, 1996.
[2] P. Blanchard, C. Lamonier, A. Griboval, E. Payen, Appl. Catal. A: Gen. 322 (2007) 33.
[3] P. Blanchard, C. Mauchaussee, E. Payen, J. Grimblot, O. Poulet, N. Boisdron, R. Loutaty, Stud. Surf. Sci. Catal. 91 (1995) 1037.
[4] P. Blanchard, E. Payen, J. Grimblot, O. Poulet, R. Loutaty, Stud. Surf. Sci. Catal. 111 (1997) 211.
[5] Y. Yoshimura, T. Sato, H. Shimada, N. Matsubayashi, M. Imamura, A. Nishijima, M. Higo, S. Yoshitomi, Catal. Today 29 (1996) 221.
[6] Y. Yoshimura, N. Matsubayashi, T. Sato, H. Shimada, A. Nishijima, Appl. Catal. A: Gen. 79 (1991) 145.
[7] K. Inamura, K. Uchikawa, S. Matsuda, Y. Akai, Appl. Surf. Sci. 121/122 (1997) 468.
[8] R. Iwamoto, N. Kagami, A. Iino, J. Jpn. Petrol. Inst. 48 (4) (2005) 237.
[9] R. Iwamoto, N. Kagami, Y. Sakoda, A. Iino, J. Jpn. Petrol. Inst. 48 (6) (2005) 351.
[10] G. Kishan, L. Coulier, V.H.J. de Beer, J.A.R. van Veen, J.W. Niemantsverdriet, J. Catal. 196 (2000) 180.
[11] L. Coulier, G. Kishan, J.A.R. van Veen, J.W. Niemantsverdriet, J. Vac. Sci. Technol. A 19 (4) (2001) 1015.
[12] L. Coulier, V.H.J. de Beer, J.A.R. van Veen, J.W. Niemantsverdriet, J. Catal. 197 (2001) 26.

[13] G. Kishan, J.A.R. van Veen, J.W. Niemantsverdriet, Top. Catal. 29 (2004) 103.
[14] G. Kishan, L. Coulier, V.H.J. de Beer, J.A.R. van Veen, J.W. Niemantsverdriet, J. Chem. Soc., Chem. Commun. (2000) 1103.
[15] R. Cattaneo, Th. Weber, T. Shido, R. Prins, J. Catal. 191 (2000) 225.
[16] S.P.A. Louwers, R. Prins, J. Catal. 133 (1992) 94.
[17] G. Kishan, L. Coulier, J.A.R. van Veen, J.W. Niemantsverdriet, J. Catal. 200 (2001) 194.
[18] L. Coulier, G. Kishan, J.A.R. van Veen, J.W. Niemantsverdriet, J. Phys. Chem. B 106 (2002) 5897.
[19] R. Cattaneo, T. Shido, R. Prins, J. Catal. 185 (1999) 199.
[20] R. Cattaneo, F. Rota, R. Prins, J. Catal. 199 (2001) 318.
[21] M. Sun, D. Nicosa, R. Prins, Catal. Today 86 (2003), 173 and references therein.
[22] J.A.R. van Veen, E. Gerkema, A.M. van der Kraan, A. Knoester, J. Chem. Soc., Chem. Commun. (1987) 1684.
[23] D. Nicosa, R. Prins, J. Catal. 229 (2005) 424.
[24] D. Nicosa, R. Prins, J. Catal. 234 (2005) 414.
[25] N. Frizi, Thesis, Lille, France 2004.
[26] T. Yasuhito, S. Shigeru, I. Yoshimasa, E. Patent 0506206 (1992).
[27] M.J. Ledoux, C.P. Huu, Y. Segura, F. Luck, J. Catal. 121 (1990) 70.
[28] L. Benoist, D. Gonbeau, G. Pfister-Guillouzo, E. Schmidt, G. Meunier, A. Levasseur, Thin Solid Films 258 (1995) 110.
[29] J. Grimblot, pHD, Lille, France, 1977.
[30] H.J. Scofield, J. Electron. Spectrosc. Relat. Phenom. 8 (1976) 129.
[31] P. Beccat, P. Da Silva, Y. Huiban, S. Kaztelan, Oil Gas Sci. Techn. Rev. IFP 54 (4) (1999) 487.
[32] B. Ravel, M. Newville, Phys. Scr. T115 (2005) 1007.
[33] A. Cervilla, A. Llopis, J.A. Ramírez, A. Doménech, P. Palanca, M.T. Pilcher, C.A. Guilardi, A. Orlandini, J. Chem. Soc., Dalton Trans. (1994) 175.
[34] W. Yang, C. Lu, S. Lu, H. Zhuang, Helvet. Chim. Acta 85 (2002) 2417.
[35] J.F. Martin, J.T. Spence, J. Phys. Chem. 74 (1970) 3589.
[36] S. Patai (Ed.), The Chemistry of Thiols, John and Sons, 1974.
[37] R.H. Lana, L.E. Bennet, J. Am. Chem. Soc. 92 (4) (1970) 1089.
[38] S. Kasztelan, J. Grimblot, J.P. Bonnelle, E. Payen, H. Toulhoat, Y. Jacquin, Appl. Catal. 7 (1983) 91.
[39] C.B. Bloodworth, B. Demetriou, R. Grzeskowiak, Inorg. Chim. Acta 53 (1981) L85–L87.
[40] S.N. Rao, K.N. Munshi, N.N. Rao, M.M. Bhadbhade, E. Suresh, Polyhedron 18 (1999) 2491.
[41] D. Coucouvanis, A. Toupadakis, J.D. Lane, S.M. Koo, C.G. Kim, A. Haddjikyriacou, J. Am. Chem. Soc. 113 (1991) 5271.
[42] W.E. Newton, J.L. Corbin, J.W. McDonald, J. Chem. Soc., Dalton Trans. (1973) 1044.
[43] W.E. Newton, J.L. Corbin, D.C. Bravard, J.E. Searles, J.W. McDonald, Inorg. Chem. 13 (5) (1974) 1100.
[44] A. Królikowska, A. Kudelski, A. Michota, J. Bikowska, Surf. Sci. 532–535 (2003) 227.
[45] N. Frizi, P. Blanchard, E. Payen, J.P. Dath, in press.
[46] E. Payen, S. Kastelan, S. Houssenbay, R. Szymanski, J. Grimblot, J. Phys. Chem. 93 (1989) 6501.
[47] T.G. Parham, R.P. Merrill, J. Catal. 85 (1984) 295.
[48] R.G. Leliveld, A.J. van Dillen, J.W. Geus, D.C. Koningsberger, J. Catal. 165 (1997) 184.
[49] R.G. Leliveld, A.J. van Dillen, J.W. Geus, D.C. Koningsberger, J. Catal. 171 (1997) 115.
[50] C. Geantet, Y. Soldo, C. Glasson, N. Matsubayashi, M. Lacroix, O. Proux, O. Ulrich, J.L. Hazemann, Catal. Lett. 73 (2001) 95.
[51] I. Alstrup, I. Chorkendoff, R. Candia, B.S. Clausen, H. Topsøe, J. Catal. 77 (1982) 397.
[52] R. Candia, O. Sorensen, J. Villadsen, N.Y. Topsøe, B.S. Clausen, H. Topsøe, Bull. Soc. Chim. Belg. 93 (1984) 763.
[53] H. Schweiger, P. Raybaud, H. Toulhoat, J. Catal. 212 (2002) 33.
[54] S.L. Gonzalez-Cortés, T.-C. Xiao, P.M.F.J. Costa, B. Fontal, M.L.H. Green, Appl. Catal. A: Gen. 270 (2004) 209.